PREPRINT UCRL-78429

CONF-761108--12

Lawrence Livermore Laboratory

HOLOGRAPHIC INTERFEROMETRY OF LASER FUSION TARGETS AT 2660 Å

L. W. Coleman, D. T. Attwood and D. W. Sweeney

September, 1976

This paper was prepared for presentation at the American Physical Society, 1976 Annual Meeting of the Division of Plasma Physics, November 15-19, 1976 San Francisco, CA

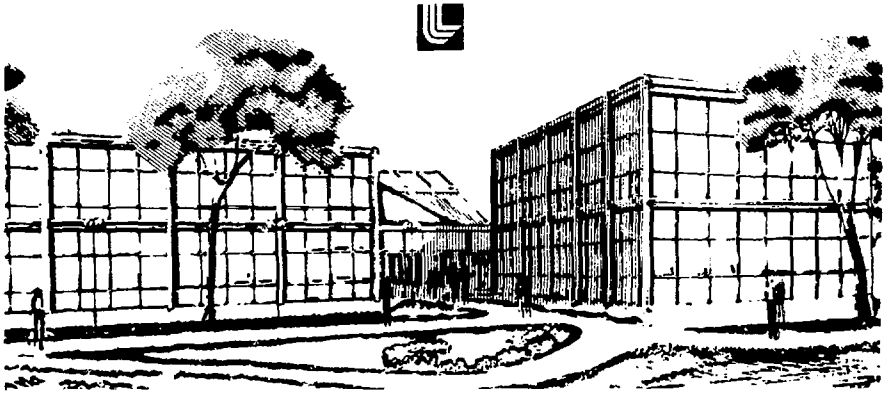

HOLOGRAPHIC INTERFEROMETRY OF LASER FUSION TARGETS AT 2660 Å*

L. W. Coleman, D. T. Attwood and J. W. Sweeney
Lawrence Livermore Laboratory, University of California
Livermore, California 94550

Abstract

Holographic interferometry at 2660 Å has been used to study plasma blowoff from 80 micron diameter laser fusion targets. Scale lengths of 11 microns, measured with 1 micron spatial resolution, are recorded at 7 X 10^{20} e/cc after 800 psec of hydrodynamic expansion. These results suggest much steeper density gradients at peak irradiation intensity. The observed fringe pattern is strongly dependent on interferometric imaging, as expected for strong transverse gradient refractive media. Significant interpretive errors, which might occur in a single image classical interferometer, are avoided with this holographic technique.

Introduction

The plasma atmosphere surrounding targets irradiated by sub-nanosecond Nd laser pulses is of interest to the laser fusion program[1,2] because it is here that energy is absorbed and transported to the core region. Optical probing of the target atmosphere is a powerful diagnostic tool that can be used to characterize this important region. This technique can be used to determine electron density distributions in the 10^{20} to 10^{21} e/cc range. Typical target/laser interactions of present interest to the laser fusion program involve 100 μm diameter targets irradiated by 100 picosecond, 1.06 μm pulses with laser intensities on target of 10^{14} to 10^{16} W/cm^2. In these situations, axial scale lengths for electron density are in the 1-20 μm range, and critical density contours move with velocities from zero to greater than 10^7 cm/sec, depending on target wall thickness, time of observation, and characteristics of the irradiating pulse.

Figure 1 shows the basic scheme in which an irradiated target is probed transversely to determine optical properties of the surrounding plasma atmosphere. Typical observations include phase velocity, rotation of the polarization vector, and refractive turning. These in turn provide measures of local electron density via interferometry, magnetic field intensity via Faraday rotation, and critical density contour motion via shadowgraphs.[3] For these probing measurements, the most significant limitation is that due to refractive turning in the steep gradient density field. A simple example serves to illustrate the strong wavelength dependence of this effect. We consider target irradiation with wavelength λ_0, resulting in an electron density distribution which is Gaussian in the transverse direction and exponentially decaying on axis, i.e.,

$$n(\underline{r}) = n_c \, e^{-8Z^2/L^2} \, e^{-x/\ell} \qquad (1)$$

*Work performed under the auspices of the U. S. Energy Research and Development Administration, contract No. W-7405-Eng-48.

EP

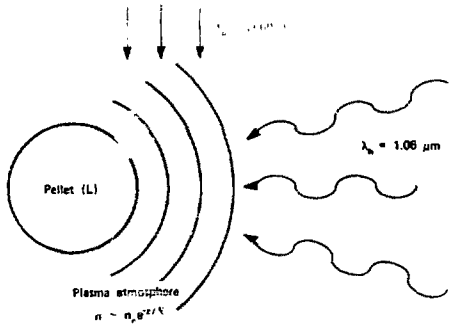

Fig. 1. Optical probing of laser irradiated target with a 2660 Å probe pulse.

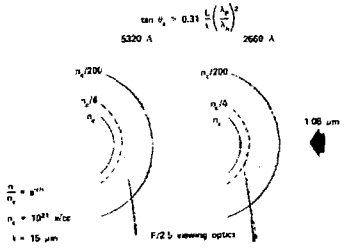

Fig. 2. Refractive turning of optical probe pulses at differing wavelengths, demonstrating the wavelength squared advantage of an ultraviolet probe.

where L is the $1/e^2$ transverse diameter and ℓ is the on-axis "scale length." If this distribution is probed transversely with a wavelength λ_p, as described in Fig. 1, simple arguments show that in passing through the critical region (for λ_h) the probe pulse is refractively turned through an angle θ given by[4]

$$\tan \theta = (0.313) \frac{L}{\ell} \left(\frac{\lambda_p}{\lambda_h}\right)^2 \qquad (2)$$

The crucial dependence of turning angle on wavelength ratio is evident in Eq. (2). For a 1.06 μm "heating" pulse, it is clearly advantageous to use a probe wavelength in the middle ultraviolet. The severity of the problem is evidenced by a numerical example in which we take a transverse dimension L = 100 μm, an axial scale length ℓ = 10 μm, and use a frequency quadrupled probe pulse such that $(\lambda_p/\lambda_h) = 1/4$. In this case Eq. (2) predicts a refractive turning angle of approximately 11°. Observation of such a probe pulse in any of the above mentioned diagnostic schemes, requires viewing optics with an effective F/2.5 aperture. Large aperture collection optics such as this clearly require correction for spherical aberration. A further description of the λ^2 refractive behavior is shown in Fig. 2, where computer ray traces are presented for frequency doubled and quadrupled probe pulses. Only those rays collected by the F/2.5 viewing optics are shown. Even with this relatively shallow gradient, ℓ = 15 μm, the 5320 Å cannot collect information describing the critical region; the 2660 Å probe is absolutely required in this parameter range.[5]

In response to the above observations we have set out to develop a probing capability in the middle ultraviolet. The method of production is schematicized in Fig. 3, where one observes the successive use of KDP and ADP crystals to double and redouble a split off sample of a 1.064 μm irradiation pulse. The resultant 2660 Å pulse has been used to probe transversely at a variety of delay times

between -100 and +800 picoseconds. For a 150 ps FWHM irradiation pulse, the probe pulse duration is approximately 100 ps.[6] Efforts are under way to shorten this further. Efficient energy conversion[7] to these harmonics permits us to obtain probe intensities as high as 10^{10} W/cm^2 at the target, a value which is required for some applications involving Faraday rotation. The 100 ps, 2660 Å probe has been used in our laboratory for all three of the basic measurement techniques discussed: interferometry, Faraday rotation, and shadowgraphs.

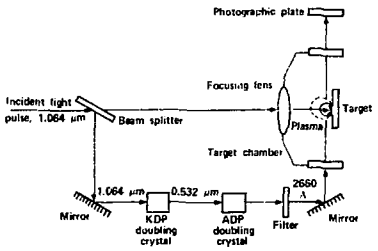

Fig. 3. Schematic diagram showing how a synchronous, frequency quadrupled probe pulse is obtained. Both frequency doubling processes occur with a high energy conversion efficiency.

Interferometry

The understanding of optical absorption by laser produced plasmas requires a knowledge of electron density distributions in the critical region. The axial scale length for density decay plays a crucial role in determining which of several competing mechanisms account for the absorption and reflection of incident laser light. Because the refractive index is simply related to free electron concentration[8,9] in these highly ionized plasmas, interferometry can be used to unambiguously determine the density distribution. For the plasma model described in the introduction, one determines a required spatial resolution for the interferometer in terms of fringe spacing at 10^{21} e/cc, to be

$$\Delta Z)_{\text{resolution}} \simeq \frac{3\ell\lambda_h^2}{L\lambda_p} \tag{3}$$

or approximately 1.5 μm for the parameters described below Eq. (2). Because the contours of constant electron density (refractive index) move with high velocity, one is required to use a sufficiently short duration probing pulse, which is given to first order by

$$\Delta\tau)_{\text{resolution}} \leq \frac{\Delta Z)_{\text{res}}}{2\overline{V}_c} \tag{4}$$

where $\overline{V}_c$ is the velocity of the critical density contour (10^{21} e/cc) during passage of the probe pulse. For probe pulse durations greater than that described in Eq. (4), the interferometric fringes will smear, lose contrast, and eventually be lost. For contour velocities in the 10^6 to 10^7 cm/sec range, one requires probe pulse durations of 100 to 10 ps, respectively. Slower velocities can be obtained by irradiating thin walled targets and probing them during reversal of contour motion ($\overline{V}_c \approx 0$).

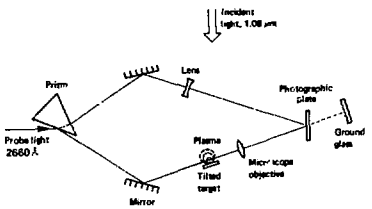

Fig. 4. High resolution holographic interferometer. With a wavelength of 2660 Å and F/2.5 collection optics, this system provides a spatial resolution of approximately 1 μm.

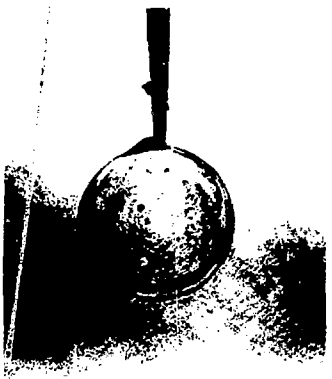

Fig. 5. Reconstruction of a single exposure hologram of an unirradiated 80 μm diameter glass microballoon. The hologram was made at 2660 Å with a 100 psec exposure time. The hologram was reconstructed with cw He-Ne laser.

The interferometer we use is shown in Fig. 4. It is holographic in nature, provides the required spatial resolution, and permits simple and accurate imaging, factors of great importance for studying strongly refracting density fields. Figure 5 shows a reconstruction from a single exposure hologram, made for reference imaging purposes, of an 80 μm diameter glass shell before irradiation. The hologram was made with a single 100 ps, 2660 Å pulse, and reconstructed with a cw He-Ne laser. Diffraction rings with a separation of 1.5 μm are evident. Figure 6 shows the same target 800 ps after irradiation from the left by a 1/4 J, 150 ps Nd laser pulse. Target intensity of the 1.06 μm heating pulse was approximately 10^{14} W/cm^2. Again 100 ps, 2660 Å pulses were used, this time in the double pulse mode. The time between exposures was 5 minutes. It is evident from Fig. 6 that this target was hit 12 μm low, and that as a result the blow off is not coaxial with that of the heating laser pulse. Note also that the irradiated side shows a flat fringe field, while the far side appears to blow off in a more isotropic manner. This is presumably due to radiative forces which exist on the irradiated side during the period of high laser intensity. Abel inversion of the flat field fringes indicates a peak electron density of 7 x 10^{20} e/cc with an axial scale length at the density of 11 μm. Since this data is obtained after a delay of 800 ps, a time during which hydrodynamic expansion is known to play a significant role, we can assume that the scale length was considerably shorter during the period of peak laser heating. Higher electron densities were not observed here because of temporal smearing of fringe data. Since a 100 ps probe pulse was used, we can estimate that the contour velocity was approximately 2 x 10^6 cm/sec. Efforts to reduce the probe pulse duration are presently under way. When successful, this will permit us to study electron densities in excess of 10^{21} e/cc.

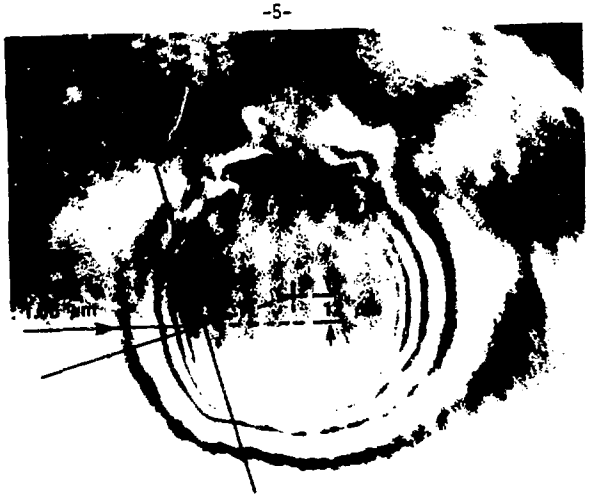

Fig. 6. Reconstruction of a double exposure hologram of the same target shown in Fig. 5. The second exposure was made 800 ps after irradiation by a 1.06 μm laser heating pulse.

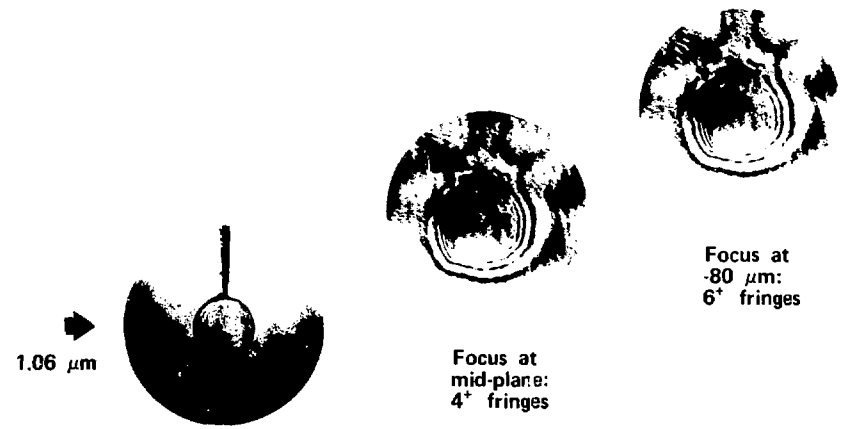

Fig. 7. The importance of image plane accuracy is demonstrated for interferometry of strongly refracting plasmas. The reconstructions in the center (reference position) and to the right (-80 μm image plane displacement)aare from the same hologram.

Because the probe pulse is strongly refracted in passing through the higher density regions of the plasma (See Eq. 2), it exits at an angle significantly different from that of a reference ray traversing the same initial ray path in vacuum. As a consequence, imaging accuracy plays a very significant role. Additional fringes appear as one images further and further behind the mid-plane of the plasma (away from the collecting lens). Figure 7 shows the effect of imaging plane. Figures 7a and 7b are imaged on the initial support stalk of the ball. Figure 7c, reconstructed from the same hologram as 7b, shows the effect an 80 μm imaging error would have in a conventional (non-holographic) interferometer. The additional fringes are due only to the non-collinear nature of object and reference beams, do not indicate higher electron density, but could mislead one to believe that densities in excess of 10^{21} e/cc were recorded had they been observed in a conventional manner.

Conclusions

We have described a technique for studying electron density distribution in laser produced plasmas. It is clear that for these techniques it is necessary to have large aperture corrected optics, and that probe pulses in the middle ultraviolet be used. Given these restraints, we have described the spatial and temporal resolutions required for meaningful experiments. Results with 100 ps duration, 2660 Å probe pulses have been presented for techniques involving holographic interferometry. To our knowledge, these are the only reported measurements of plasma densities at this short wavelength, and further, they have resulted in the highest interferometrically determined electron densities (to 7×10^{20} e/cc) reported to date. The density scale length of 11 μm measured with a resolution of 2 μm, is as short as any direct measurement reported and the only observation with this degree of spatial resolution. The importance of accurate imaging has been noted by way of demonstration (Fig. 7) for interferometry of strongly refracting plasmas. The results presented here show that observed fringe patterns vary significantly with image plane and can therefore lead to large errors if misinterpreted.

Acknowledgments

The authors acknowledge the excellent technical assistance of E. L. Pierce in all experimental phases of this project.

References

1. Nuckolls, J., Wood, L., Thiessen, A., and Zimmerman, G., Nature 239, 139 (1972).
2. Emmett, J. L., Nuckolls, J., and Wood, L., Sci. Amer. 230, 24 (1974).
3. Attwood, D. T., Ultraviolet Probing of Laser Produced Plasmas With Picosecond Pulses, XII Int'l. Cong. High Speed Photog., Toronto, Canada, Aug. 1976; UCRL 77744.
4. Attwood, D. T., Coleman, L. W., and Sweeney, D. W., Appl. Phys. Lett. 26, 616 (1975).
5. Sweeney, D. W. Attwood, D. T., and Coleman, L. W. Appl. Opt. 15, 1126 (1976).
6. Attwood, D. T., Pierce, E. L., and Coleman, L. W. Opt. Commun. 15, 10 (1975).
7. Attwood, D. T., Bliss, E. S. Pierce, E. L., and Coleman, L. W., IEEE J. Quant. Elec. 12, 203 (1976).

8. For the plasmas of interest here one can approximate the refractive index by

$$\kappa(\underline{r}) = 1 - \frac{1}{2}\frac{n(\underline{r})}{n_c}\left(1 \pm \frac{\omega_c}{\omega}\right)$$

where n(r) is the electron concentration, $n_c = 1.6 \times 10^{22}$ e/cc, ω is the radian frequency of the probe, and ω_c is the magnetic field dependent electron cyclotron frequecy. For the parameters of interest here one typically has

$$10^{-2} < \frac{n}{n_c} < 10^{-1} \text{ and } 10^{-3} < \frac{\omega_c}{\omega} < 10^{-2}.$$

9. Clemmow, P. C. and Dougherty, J. P., Electrodynamics of Particles and Plasmas (Addison-Wesley, Reading, Mass., 1969), Ch. 5.